

# *Through-thickness thermal conduction in glass fiber polymer–matrix composites and its enhancement by composite modification*

**Yoshihiro Takizawa & D. D. L. Chung**

**Journal of Materials Science**

Full Set - Includes 'Journal of Materials  
Science Letters'

ISSN 0022-2461

Volume 51

Number 7

J Mater Sci (2016) 51:3463-3480

DOI 10.1007/s10853-015-9665-x



**Your article is protected by copyright and all rights are held exclusively by Springer Science +Business Media New York. This e-offprint is for personal use only and shall not be self-archived in electronic repositories. If you wish to self-archive your article, please use the accepted manuscript version for posting on your own website. You may further deposit the accepted manuscript version in any repository, provided it is only made publicly available 12 months after official publication or later and provided acknowledgement is given to the original source of publication and a link is inserted to the published article on Springer's website. The link must be accompanied by the following text: "The final publication is available at [link.springer.com](http://link.springer.com)".**

# Through-thickness thermal conduction in glass fiber polymer–matrix composites and its enhancement by composite modification

Yoshihiro Takizawa<sup>1</sup> · D. D. L. Chung<sup>1</sup>

Received: 15 September 2015 / Accepted: 11 December 2015 / Published online: 21 December 2015  
© Springer Science+Business Media New York 2015

**Abstract** Continuous glass fiber polymer–matrix composites are electrically insulating and used for printed wiring boards, but their thermal conductivity needs to be increased without sacrificing the electrical insulation ability. The through-thickness thermal conductivity of these epoxy–matrix composite laminates with in-plane fibers is found to be effectively modeled using the Rule of Mixtures with fibers and matrix mainly in parallel in the through-thickness direction, in contrast to the series model that is effective for previously studied carbon fiber composites. For the glass fiber composites, the through-thickness conductivity is similar to the in-plane conductivity. The conductivity for woven fiber composites is increased by up to 80 % by curing pressure increase (from 0.69 to 4.0 MPa), up to 50 % by solvent (toluene or ethanol) treatment of the prepreg for partial surface resin removal, and up to 90 % by boron nitride nanotube (BNNT) incorporation along with solvent treatment. The highest through-thickness thermal conductivity reached is 1.2 W/(m K), which is higher than those of all prior reports on glass fiber composites. The interlaminar interfaces are negligible in through-thickness thermal resistance compared to the laminae, as for previously studied carbon fiber composites. The fiber contribution dominates the lamina resistance. The fiber–fiber interface contribution to the lamina resistance decreases significantly with curing pressure increase or composite modification involving BNNT incorporation or solvent treatment of the prepreg.

## Introduction

Polymer–matrix composites with continuous glass fibers are important for lightweight structural applications, including wind turbines, automobile body, boats, concrete structural repair, bridge decks, and oil pipelines. Due to their electrical insulation ability, they are also used for printed wiring boards and electrical insulation. However, they exhibit low thermal conductivity. Thermal conduction is important for heat dissipation, which is one of the most critical issues that limit the performance, power, and further miniaturization of microelectronics and light-emitting diodes. With the continuous fibers in the plane of the composite panel, in-plane thermal conduction is important for heat spreading, while through-thickness thermal conduction is important for heat removal, particularly when a planar heat sink is used. Increased thermal conductivity is also desired for temperature gradient reduction (hence thermal stress reduction) and thermal fatigue resistance enhancement.

There is considerable prior work on increasing the thermal conductivity of polymers by using fillers in the absence of continuous fibers. These fillers include boron nitride (BN) particles [1, 2], graphite flakes [3], silicon carbide particles [2, 3], silicon nitride particles [2], alumina particles [2], and aluminum particles [4]. However, the science is quite different and little addressed when continuous fibers are present. This is because the continuous fibers are the major constituent (typically  $\geq 50$  vol%) in the composite and are aligned. Moreover, the continuous glass fibers are in the form of plies (laminae) and are more thermally conductive than the polymer matrix. As a result, a simple model in which the fibers are unidirectional and perfectly aligned, with no fiber–fiber contact, would point to anisotropy in the thermal conductivity, such that the

✉ D. D. L. Chung  
ddlchung@buffalo.edu

<sup>1</sup> Composite Materials Research Laboratory, University at Buffalo, State University of New York, Buffalo, NY 14260-4400, USA

conductivity is higher in the in-plane direction than the through-thickness direction. Indeed, the thermal conductivity of FR-4 (a woven glass fiber epoxy–matrix composite that is commonly used for printed wiring boards and that includes a flame retardant, which is typically bromine) is higher in the in-plane direction (0.81 W/(m K)) than the through-thickness direction (0.29 W/(m K)) [5], though the degree of anisotropy in the thermal conductivity is not high. It was also reported that continuous glass fiber polymer–matrix composites exhibit anisotropic electrical conductivity with the electrical conductivity being higher in the in-plane direction than the through-thickness direction [6]. In contrast to the abovementioned reports of anisotropy, the essential absence of thermal conductivity anisotropy occurs in aligned short glass fiber polymer–matrix composites, with the explanation in terms of the isotropy within a glass fiber [7]. This unexpected result on isotropy indicates the need to study continuous glass fiber composites, which have the fibers more clearly aligned than the short fiber composites of this prior work [7]. In relation to the continuous fiber composites, the science of the through-thickness conduction is more complex than that of the in-plane conduction; the latter is simpler because it is dominated by conduction along the axis of the fibers, whereas the former involves contributions from the fibers, matrix, and fiber–matrix interface. Thus, this paper is focused on the science behind the thermal conduction in continuous glass fiber composites in the through-thickness direction.

In order to improve the thermal conductivity of glass fiber polymer–matrix composites, carbon nanotubes (CNTs) [8, 9] and carbon nanofibers [10] have been added to the matrix. The combined use of carbon fibers and glass fibers [11] and the stitching of continuous copper wire [12] are other methods that have been used. However, all these methods [8–12] involve the addition of an electrically conductive constituent, which would cause the composite to lose its electrical insulation ability. For printed wiring boards, it is desirable to increase the thermal conductivity without increasing the electrical conductivity.

Prior work on the modeling of the thermal conductivity of composite materials has addressed those with fillers in the absence of continuous fibers. Examples of such modeling include consideration of the dispersed phase as consisting of spheres in cubic arrangements [13], consideration of a tetragonal array of spheroids [14], the use of the equivalent inclusion method and the finite element method [15], the use of the finite element method based on the resistor networks approach [16], consideration of the filler size distribution law [17], the use of the effective medium theory [18], and the use of the asymptotic expansion homogenization approach [19]. In relation to continuous fibers, modeling work has involved the variational

approach [20] and the combination of series and parallel models [21].

Both the in-plane [8, 9, 22] and through-thickness [10–12, 22] directions are relevant to thermal conduction applications. This work addresses the through-thickness conductivity. In spite of the prior work [8–12, 22], the mechanism of conduction has not been adequately addressed. In particular, the role of the interlaminar interface and that of the fiber–fiber contacts within a lamina have not been addressed.

Prior work [23] has addressed the through-thickness thermal conductivity of continuous carbon fiber polymer–matrix composites and reported that the through-thickness thermal resistance is dominated by the laminae rather than the interlaminar interfaces in the laminate. Furthermore, it was reported that the through-thickness thermal conductivity is increased by up to 60 % by raising the curing pressure from 0.1 to 2.0 MPa and up to 33 % by incorporation of a filler ( $\leq 1.5$  vol%) at the interlaminar interface [23]. Due to the high thermal conductivity of carbon fibers compared to glass fibers, these results on carbon fiber composites point to the need to extend the work to glass fiber composites.

Since fillers that are electrically and thermally conductive are much more common than those that are electrically insulating but thermally conductive, the choice of fillers is wider for carbon fiber composites (which are electrically conductive anyway) than glass fiber composites (which are to remain electrically insulating, as required for printed circuit boards, etc.). Thus, in contrast to prior work that uses electrically conductive fillers [8–10, 23], this work uses an electrically non-conductive filler.

The scientific objectives of this work are (i) to increase the through-thickness thermal conductivity of glass fiber composites without affecting the electrical insulation ability, and (ii) to clarify the mechanism of through-thickness thermal conduction in glass fiber composites. In contrast to prior work [8–10, 23], which uses electrically conductive fillers, an electrically insulating filler is used in this work.

BN is known for its combination of high thermal conductivity and electrical non-conductivity. Hexagonal BN is isoelectronic to graphite and is the most stable and softest among BN polymorphs. It is commonly in particulate or flake form. The BN nanotube (BNNT) is similar in structure to the CNT. Compared to the particulate form of BN, BNNT is attractive for its large aspect ratio, which helps the attainment of connectivity in thermal conduction.

The BNNTs have received considerable recent attention due to their combination of electrical non-conductivity, high thermal conductivity, low dielectric constant, and high modulus of elasticity [24–26]. At room temperature, the thermal conductivity of a multi-walled BNNT can be

comparable to that of a multi-walled CNT and may exceed it if it is made isotopically pure [26]. BNNT and CNT are structural analogs. The main difference between BNNTs and CNTs is that BNNTs are electrically nonconductive, whereas CNTs are electrically conductive. The combination of low electrical conductivity and high thermal conductivity is not common among materials; diamond is the primary example of a material that exhibits this combination of properties. This combination of properties is valuable for heat dissipation from microelectronic packages, which commonly suffer from overheating.

Another attractive property of BNNTs is a relatively low value of the relative dielectric constant (the real part); a value of 5.90 has been predicted by calculation [24]. The combination of high thermal conductivity and a low value of the relative dielectric constant is not common among electrically nonconductive materials. Polymers tend to have low values of the relative dielectric constant, but relatively low values of the thermal conductivity; ceramics tend to have higher thermal conductivity, but also higher values of the relative dielectric constant. Applications of electrical insulators in electronic packaging include encapsulations, interlayer dielectrics, printed circuit boards, and electric cable jackets. With heat dissipation and a high signal propagation speed being critically important for enhancing the reliability, power, performance and further miniaturization of microelectronics, materials with high thermal conductivity, low dielectric constant, and low electrical conductivity are much needed.

## Experimental methods

### Materials

Glass fiber epoxy–matrix composite specimens are fabricated by hand lay-up and compression molding of a stack of prepreg sheets. The molding is performed at 120 °C (250 °F) for 120 min, as recommended by the prepreg manufacturers; the molding (curing) pressure ranges from 0.69 to 4.0 MPa. Two types of prepreg are used, namely a biaxially woven (eight harness satin weave) prepreg and a nonwoven unidirectional prepreg (25 fibers stacked). The pressure of 0.69 MPa is at the high ends of the pressure ranges recommended by the manufacturers of both the nonwoven and woven prepreps. The nonwoven prepreg is used to make unidirectional and crossply composites. Basic information on the two types of prepreg is shown in Table 1; that on the corresponding two types of glass fiber is shown in Table 2. The thermal conductivity values of glass and epoxy are 1.3 and 0.19 W/(m K), respectively, for the woven prepreg and are 1.45 and 0.22 W/(m K), respectively, for the aligned fiber prepreg.

For a modified form of the composite, the prepreg is treated with a solvent (either ethanol or toluene) prior to its use. In the treatment, each layer of prepreg is separately immersed in a bath of ethanol for 3 s. The prepreg sheet is then removed from the bath and placed on a PTFE-coated glass-fiber fabric sheet. After this, the vehicle in the sheet is allowed to evaporate in air at room temperature for 24 h. Once the prepreg sheets have dried separately, they are stacked to reach the number of laminae desired. This modification of the composite is aimed at reducing the amount of excess resin on the prepreg surface, thereby decreasing the matrix volume fraction.

The BNNT material is provided by BNNT, LLC (Newport News, VA). The tubes are synthesized using the high temperature/high pressure (HTP) method, also called the pressurized vapor/condenser (PVC) method. This method produces highly flexible, high aspect ratio BNNTs with high crystallinity. According to the manufacturer, the number of walls in a nanotube typically ranges from 1 to 5, with 2 and 3 being the most common. The tube length is up to 200 μm. The specific surface area is up to 300 m<sup>2</sup>/g. There are up to 5 BNNTs across each BNNT bundle. The purity is up to 40–50 wt%. The impurities are in the form of hexagonal BN flakes and elemental boron microdroplets. The as-grown material has a cotton-like appearance, with an unusually low tap density of about 0.25 mg/cm<sup>3</sup>. The true density is taken to be 2.38 g/cm<sup>3</sup>, which is the theoretical value for single-walled BNNT [27]. The energy band gap is 5.7 eV, according to the manufacturer. A scanning electron microscope (SEM) image of the BNNTs is shown in Fig. 1. In spite of the particulate impurities, the structure is vastly dominated by the nanotubes.

The incorporation of BNNTs in a composite is conducted by immersing the prepreg in a bath of a dispersion of BNNTs (0.021 wt%) in toluene for 3 s. Ethanol does not disperse BNNTs as well as toluene. The immersion causes the deposition of BNNTs on the prepreg surface, in addition to slight removal of the excess resin on the prepreg surface. The prepreg sheet is then removed from the bath and placed on a polytetrafluoroethylene-coated glass-fiber fabric sheet. After this, the vehicle in the sheet is allowed to evaporate in air at room temperature for 24 h. The process of BNNT incorporation includes toluene treatment, due to the use of toluene to disperse the BNNTs.

### Density measurement

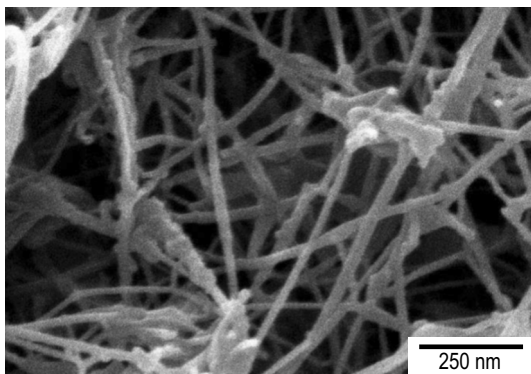
The density of a composite is measured using specimens of size 25.4 × 25.4 mm and thickness ranging from 0.38 to 1.35 mm, depending on the number of laminae. Six specimens of each type are measured. The density is used to calculate the fiber volume fraction based on the Rule of Mixtures. According to the prepreg manufacturers, the

**Table 1** Basic information on the two types of prepreg according to the prepreg manufacturers

|                                    | Nonwoven prepreg    | Woven prepreg                    |
|------------------------------------|---------------------|----------------------------------|
| Manufacturer                       | Tencate             | Park Electrochemical Corporation |
| Fiber type                         | S2 FG 200-284GSM    | 7781 E-Glass                     |
| Epoxy type                         | BT250E–1 resin      | E761                             |
| Areal weight (g/cm <sup>2</sup> )  | 0.0428 <sup>a</sup> | 0.0303                           |
| Resin content (wt%)                | 33                  | 39                               |
| Thickness (mm)                     | 0.24 <sup>a</sup>   | 0.22                             |
| Glass transition temperature $T_g$ | 125 °C              | 115 °C                           |
| Resin density (g/cm <sup>3</sup> ) | 1.17                | 1.20                             |
| Thermal conductivity (W/(m K))     | 0.22                | 0.19                             |

<sup>a</sup> Measured in this work**Table 2** Basic properties of the glass fibers in the prepreps according to the fiber manufacturers

| Fiber type                           | S2-Glass <sup>a</sup> | E-Glass <sup>b</sup>  |
|--------------------------------------|-----------------------|-----------------------|
| Diameter (μm)                        | 9                     | 7                     |
| Density (g/cm <sup>3</sup> )         | 2.46                  | 2.58                  |
| Thermal conductivity (W/(m K))       | 1.45                  | 1.3                   |
| Softening point (°C)                 | 1056                  | 846                   |
| Annealing point (°C)                 | 816                   | 657                   |
| Strain point (°C)                    | 766                   | 615                   |
| Tensile strength (GPa)               | 4.89                  | 3.45                  |
| Young's modulus (GPa)                | 86.9                  | 80.3                  |
| Elongation at break (%)              | 5.7                   | 4.8                   |
| Volume electrical resistivity (Ω cm) | $9.05 \times 10^{12}$ | $4.02 \times 10^{14}$ |
| Specific heat (J/(g K))              | 0.74                  | 0.81                  |

<sup>a</sup> Used in the nonwoven aligned fiber prepreg<sup>b</sup> Used in the woven fiber prepreg**Fig. 1** SEM photograph of a BNNT compact obtained at a pressure of 0.47 MPa

densities of the glass fibers and matrix (cured) in the nonwoven aligned fiber prepreps are 2.46 and 1.17 g/cm<sup>3</sup>, respectively, whereas those in the woven fiber prepreg are 2.58 and 1.20 g/cm<sup>3</sup>, respectively.

## Thermal conductivity measurement

Composites with 2, 3, and 4 laminae (either nonwoven unidirectional or woven) and 3, 5, and 7 laminae (non-woven crossply) are tested. More laminae are used for the crossply composite because of the need to maintain symmetry in the lay-up configuration in order to avoid specimen warpage. The 3-lamina crossply composite has lay-up configuration [0/90/0], for example.

The measurement is performed by using the Guarded Hot Plate Method, with the specimen sandwiched by two copper blocks, each with a square cross section of dimensions 25.4 × 25.4 mm. Each composite is tested at three different thicknesses. Testing at multiple thicknesses allows the thermal resistance of the specimen–copper interface to be decoupled from that of the specimen. This is a steady-state method of heat flux measurement (ASTM Method D5470). Thermal grease is present between the specimen and the copper surfaces in order to improve the thermal contact. The method is as described in prior work [23].

At equilibrium, the temperature of the hot block is 100 °C, that of the cold block is 12–25 °C, while that of the specimen top surface is 64–89 °C and the specimen bottom surface is 23–45 °C. Thus, the average temperature of a specimen is about 55 °C. The pressure perpendicular to the plane of the laminate is controlled by using a hydraulic press at a pressure of 0.46 MPa.

Specimens of three different thicknesses are tested for each composition. For each combination of composition and thickness, two specimens are tested. The testing of three thicknesses enables the decoupling of the volumetric and interfacial contributions to the thermal resistance; in this context, the interface refers to that between the specimen and a thermal contact.

## Flexural testing

Mechanical testing is performed on 11-lamina composite specimens under three-point bending up to failure, using a

hydraulic mechanical testing system (MTS Systems Corp., Eden Prairie, MN). The specimen size is  $80 \times 11 \times 2.0$  mm. The span is 58 mm. The flexural strength is the highest stress prior to failure (not necessarily the first abrupt decrease in stress in the stress–strain curve). The flexural modulus is obtained from the slope of the straight-line portion of the curve of flexural stress versus flexural strain. This portion constitutes most of each curve. The flexural ductility is the strain at failure, which is the last abrupt drop in stress in the stress–strain curve. Only one abrupt drop in stress occurs en route to failure. Five specimens of each composition are tested.

## Results and discussion

### Composite structure

A composite consists mainly of the fibers and matrix. In case of BNNT incorporation, it contains a small proportion of filler (BNNTs) as well.

For composites with negligible air void contents, the composite density  $\rho$  is given by

$$\rho = v_f \rho_f + v_m \rho_m, \quad (1)$$

$$v_f + v_m = 1, \quad (2)$$

where  $v_f$  and  $v_m$  are the volume fractions of fibers and matrix, respectively, and  $\rho_f$  and  $\rho_m$  are the densities of fibers and matrix respectively. Using Eq. (1) and (2),  $v_f$  and  $v_m$  are obtained.

Analysis of cross-sectional optical microscope photographs (Fig. 2) gives the volume fraction of air voids in each composite. Figure 3 shows that the air voids are located at interlaminar interfaces. The air voids are essentially absent in the untreated and ethanol-treated composites, but are present in the toluene-treated composite and the composite with BNNT incorporation (Table 3). The air voids are attributed to the incomplete evaporation of the toluene (boiling point = 110.6 °C) during composite fabrication. In contrast, the evaporation of ethanol (boiling point = 78.37 °C) is relatively complete.

For composites with air void contents that are not negligible, Eq. (1) applies, with

$$v_f + v_m + v_a = 1, \quad (3)$$

where  $v_a$  is volume fraction of air voids, as determined by optical microscopy of the edge surface of each composite. Using Eq. (1) and (3),  $v_f$  and  $v_m$  are obtained.

The volume fractions of the composite constituents (fibers, matrix, filler, and air, as applicable) are shown in Table 3. The fiber volume fraction is increased, and the

matrix volume fraction is decreased by the curing pressure increase for any of the composites studied. Solvent treatment tends to increase the fiber volume fraction and decrease the matrix volume fraction, such that the effect is clearer for the woven composites than the nonwoven composites. Solvent treatment using ethanol is less effective than that using toluene in increasing the fiber volume fraction and decreasing the matrix volume fraction. The BNNT (filler) volume fraction is low (0.01). Relative to the composite without BNNT but with toluene treatment, the BNNT (filler) incorporation has essentially no effect on the constituent volume fractions. The air void volume fraction is slightly larger for the composite with BNNT incorporation than the composite without BNNT but with toluene treatment. This suggests that the epoxy resin does not penetrate fully the space between adjacent BNNTs in the composite.

### Decoupled volumetric and interfacial contributions to the thermal resistivity

The thermal resistivity (with unit  $\text{m}^2 \text{K/W}$ ) is area-independent, whereas the thermal resistance (with unit  $\text{K/W}$ ) is area-dependent. If there are  $N$  laminae, there are  $N-1$  interlaminar interfaces and the thermal resistivity  $R$  of the composite is given by

$$R = NR_\ell + (N-1)R_i, \quad (4)$$

where  $R_\ell$  and  $R_i$  are the thermal resistivity of a lamina and an interlaminar interface, respectively. Their values may be determined by measuring  $R$  for different values of  $N$ .

Figure 4 shows the plot of the thermal resistivity versus thickness for the unmodified unidirectional composite fabricated at 0.69 MPa. That the plot is a straight line means that  $R = NR_\ell$  and  $R_f$  is essentially 0. The slope of this line is the inverse of the thermal conductivity. The intercept with the vertical axis at zero thickness is the thermal resistivity of the two specimen–copper interfaces together. In Fig. 4, the resistivity of the two interfaces together is  $0.0001 \text{ m}^2 \text{K/W}$  and the measured resistivity is  $0.0005 \text{ m}^2 \text{K/W}$  for the smallest of the three thicknesses. This means that the specimen resistivity for this thickness is  $0.0005 - 0.0001 = 0.0004 \text{ m}^2 \text{K/W}$ . Hence, in spite of the presence of a thermal paste at the interface, the interfacial resistivity is substantial. Through plots like Fig. 4, the interfacial and specimen contributions to the measured resistivity are decoupled. Prior work [5, 8–11] did not decouple, except for Ref. [23]. Without the decoupling, the measured resistivity would be assumed to be the specimen resistivity, which is thus overestimated, thus resulting in underestimation of the specimen conductivity.

The lamina resistivity  $R_\ell$  is obtained by dividing the specimen resistivity (with the specimen–copper resistivity

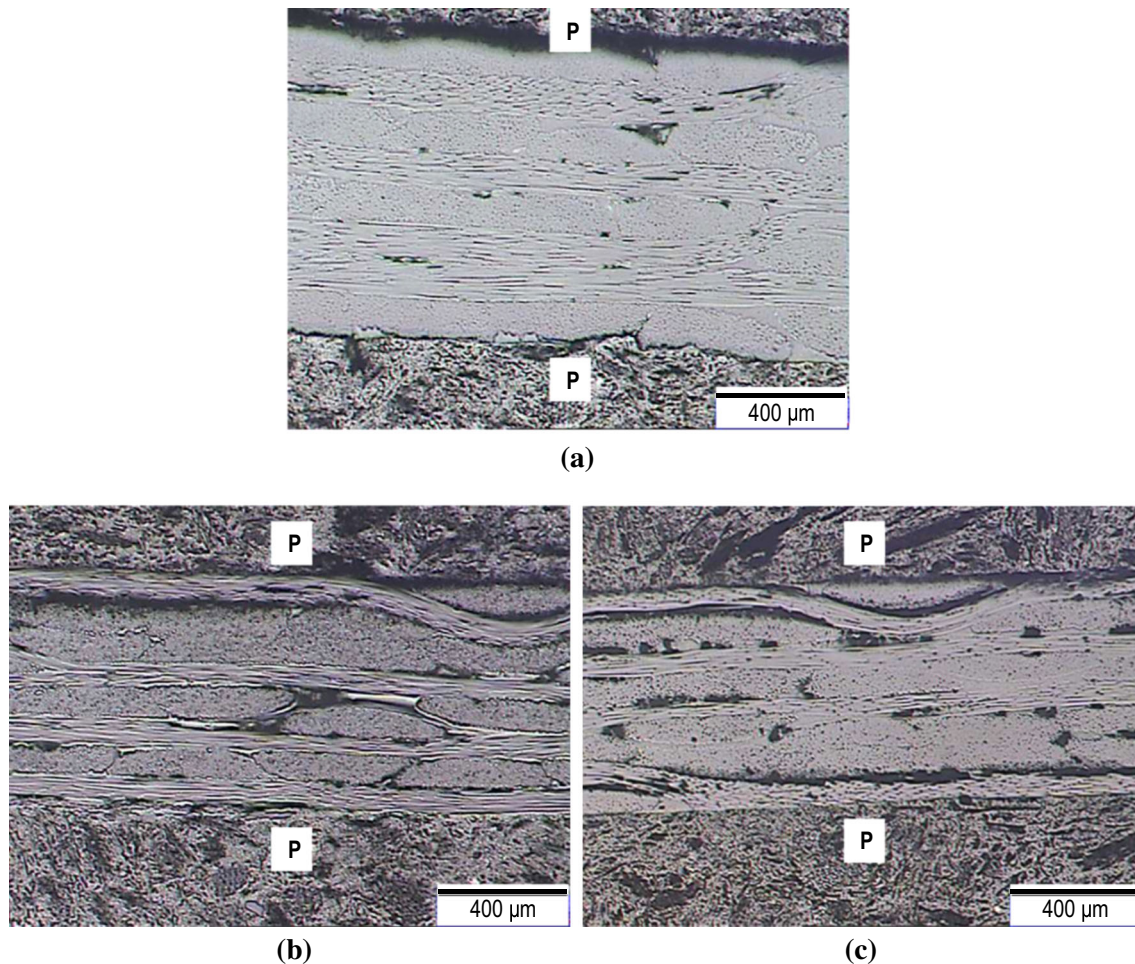


**Fig. 2** Low-magnification cross-sectional optical microscope photographs of the mechanically polished edge of four-lamina woven glass fiber epoxy–matrix composites. Each lamina includes  $0^\circ$  fibers (in the plane of the photographs) and  $90^\circ$  fibers (perpendicular to the

plane of the photographs). *Small black regions* at the interlaminar interfaces are air voids. Regions labeled P are the phenolic packing material. **a** Untreated composite. **b** Toluene-treated composite. **c** Toluene-treated composite with BNNT incorporation

excluded) by  $N$ . The finding that  $R_i$  is essentially 0 applies to all the composites and is consistent with prior work on carbon fiber composites [23]. Thus, the curing pressure and composite modification essentially do not affect  $R_i$ , which remains negligible, but they affect  $R_\ell$ .

### Thermal conductivity of composites

Since the thermal conductivity of the glass fibers is considerably higher than that of epoxy, a higher fiber volume fraction is expected to give a higher thermal conductivity. Table 3 shows that the nonwoven composites (both unidirectional and crossply composites) exhibit higher thermal conductivity than the corresponding woven composite. This is particularly clear for the usual condition corresponding to the ordinary curing pressure of 0.69 MPa and the absence of prepreg treatment. It is mostly due to the

higher fiber volume fraction of the nonwoven composites compared to the woven composite. The higher thermal conductivity of the S2 glass fiber (1.45 W/(m K), Table 2) in the nonwoven composites compared to that of the E-glass fiber in the woven composite (1.3 W/(m K), Table 2) is a minor cause, as shown by a simple calculation. This result suggests that, for applications that need a relatively high thermal conductivity, nonwoven composites are preferred to woven composites.

Table 3 shows that the solvent treatment of the prepreg enhances the thermal conductivity, density, and fiber volume fraction, whether the composite is unidirectional, crossply, or woven, and whether the solvent is ethanol or toluene. The effects of ethanol and toluene on the thermal conductivity are essentially the same. The prepreg treatment involves the removal of excess resin on the surface of the prepreg, so it is a treatment that is directed at the matrix. As a result, the matrix volume fraction is decreased

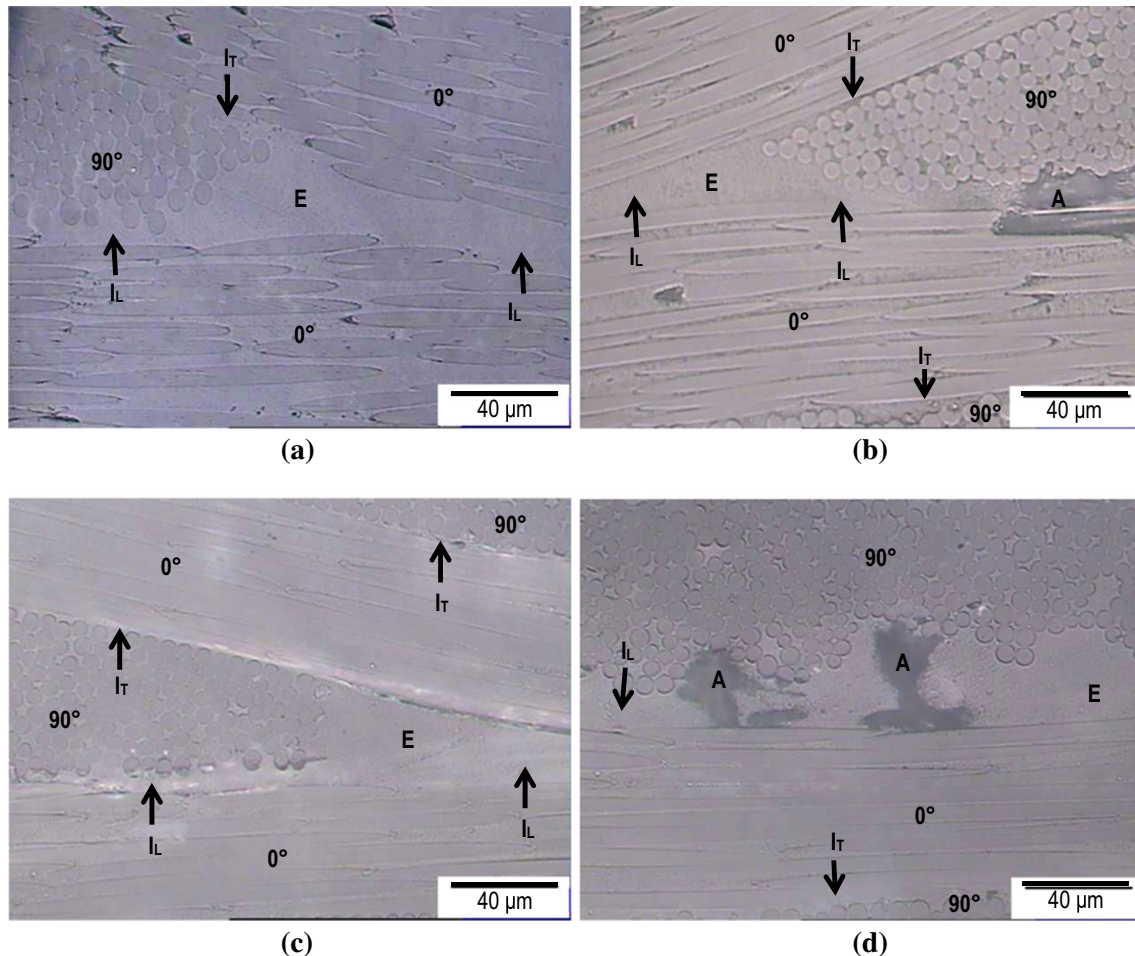


**Fig. 3** High-magnification cross-sectional optical microscope photographs of the mechanically polished edge of four-lamina woven glass fiber epoxy-matrix composites. Each photograph shows an interlaminar interface (labeled  $I_L$ ) and parts of the two associated laminae. The interlaminar interface is relatively rich in the epoxy matrix, which is labeled E. Air void regions at the interlaminar

interface are labeled A. The inter-tow interface present in a woven lamina is labeled  $I_T$ . **a** Untreated composite. **b** Toluene-treated composite. **c** Toluene-treated composite with BNNT incorporation for a region without air voids. **d** Toluene-treated composite with BNNT incorporation for a region with air voids

and the fiber volume fraction is increased by the solvent treatment.

Table 3 also shows that an increase in curing pressure enhances the thermal conductivity. The extent of resin squeeze-out during curing is greater when the curing pressure is higher. A greater extent of resin squeeze-out results in a greater increase in the extent of fiber-fiber contact in the through-thickness direction, and hence a higher through-thickness thermal conductivity.

At the highest curing pressure of 4.0 MPa, the woven unmodified composite with fiber volume fraction 0.63 exhibits through-thickness thermal conductivity 1.1 W/(m K) (Table 3). This value is below but quite close to the value of 1.3 W/(m K) for the individual fiber along its axis (Table 2). For the nonwoven unidirectional composite with fiber volume fraction 0.60 and fabricated at a curing pressure of 2.0 MPa, the through-thickness thermal

conductivity is 1.1 W/(m K) (Table 3), which is below but not far below the value of 1.45 W/(m K) for the corresponding individual fiber (Table 2). This means that the through-thickness thermal conductivity of the composites is comparable to (though smaller than) the axial thermal conductivity of the individual fiber. This supports the notion that the fiber-fiber contacts in the through-thickness direction provide an effective thermal conduction path.

The fractional increase in conductivity due to either prepreg treatment or curing pressure increase is higher for the woven composites (ranging from 44 to 76 %) than the nonwoven composites (ranging from 23 to 27 %). This is because the matrix volume fraction is higher for the woven composite (0.45) than the nonwoven composites (ranging from 0.40 to 0.42), all made at 0.69 MPa without prepreg treatment. A higher matrix volume fraction causes the prepreg treatment and the curing pressure increase to have

**Table 3** Measured and calculated thermal conductivity values for various glass fiber epoxy–matrix composites

| Fiber configuration     | Curing pressure (MPa) | Filler | Density of composite (g/cm <sup>3</sup> ) | Volume fraction |             | Air <sup>b</sup> | Measured thermal conductivity (W/(m K)) | Calculated thermal conductivity (W/(m K)) |             | p <sup>a</sup> | Fractional increase in conductivity (%) <sup>c</sup> |
|-------------------------|-----------------------|--------|---|-----------------|-------------|------------------|---|---|-------------|----------------|--|
|                         |                       |        |   | Fiber           | Matrix      |                  |   | Filler                                    | Parallel    |                |  |
| Nonwoven unidirectional | 0.69                  | No     | 1.92 ± 0.00                               | 0.58 ± 0.01     | 0.42 ± 0.01 | 0                | 0.887 ± 0.077                           | 0.93 ± 0.01                               | 0.43 ± 0.01 | 0.92 ± 0.02    | /  |
|                         | 0.69 <sup>d</sup>     | No     | 1.93 ± 0.01                               | 0.59 ± 0.01     | 0.41 ± 0.01 | 0                | 1.06 ± 0.03                             | 0.94 ± 0.01                               | 0.44 ± 0.00 | 1.2 ± 0.0      | 21 ± 14  |
| Nonwoven crossply       | 2.0                   | No     | 1.95 ± 0.00                               | 0.60 ± 0.00     | 0.40 ± 0.00 | 0                | 1.07 ± 0.17                             | 0.96 ± 0.00                               | 0.45 ± 0.00 | 1.2 ± 0.0      | 23 ± 30  |
|                         | 0.69                  | No     | 1.94 ± 0.01                               | 0.60 ± 0.00     | 0.40 ± 0.00 | 0                | 0.824 ± 0.073                           | 0.96 ± 0.01                               | 0.45 ± 0.00 | 0.73 ± 0.01    | /  |
| Woven                   | 0.69 <sup>d</sup>     | No     | 1.94 ± 0.01                               | 0.60 ± 0.00     | 0.40 ± 0.00 | 0                | 1.03 ± 0.13                             | 0.96 ± 0.02                               | 0.45 ± 0.00 | 1.2 ± 0.0      | 27 ± 27  |
|                         | 0.69 <sup>e</sup>     | No     | 1.97 ± 0.01                               | 0.62 ± 0.01     | 0.38 ± 0.01 | 0                | 1.03 ± 0.07                             | 0.98 ± 0.01                               | 0.46 ± 0.01 | 1.1 ± 0.0      | 27 ± 19  |
|                         | 0.69 <sup>d</sup>     | No     | 1.96 ± 0.02                               | 0.55 ± 0.01     | 0.45 ± 0.01 | 0                | 0.640 ± 0.041                           | 0.80 ± 0.01                               | 0.36 ± 0.01 | 0.63 ± 0.02    | /  |
|                         | 0.69 <sup>e</sup>     | No     | 2.03 ± 0.02                               | 0.60 ± 0.01     | 0.40 ± 0.01 | 0                | 0.926 ± 0.059                           | 0.86 ± 0.02                               | 0.39 ± 0.01 | 1.1 ± 0.0      | 46 ± 19  |
|                         | 0.69 <sup>f</sup>     | Yes    | 2.05 ± 0.00                               | 0.66 ± 0.00     | 0.30 ± 0.00 | 0                | 0.922 ± 0.052                           | 0.91 ± 0.00                               | 0.26 ± 0.00 | 1.0 ± 0.0      | 45 ± 18  |
|                         | 2.0                   | No     | 2.07 ± 0.00                               | 0.66 ± 0.00     | 0.28 ± 0.03 | 0.01 ± 0.00      | 1.20 ± 0.02                             | 1.1 ± 0.1                                 | 0.26 ± 0.00 | 1.1 ± 0.1      | 88 ± 15  |
|                         | 4.0                   | No     | 2.02 ± 0.01                               | 0.60 ± 0.01     | 0.40 ± 0.01 | 0                | 0.916 ± 0.012                           | 0.85 ± 0.01                               | 0.39 ± 0.01 | 1.1 ± 0.0      | 44 ± 11  |
|                         |                       | No     | 2.07 ± 0.01                               | 0.63 ± 0.01     | 0.37 ± 0.01 | 0                | 1.12 ± 0.08                             | 0.89 ± 0.01                               | 0.41 ± 0.01 | 1.5 ± 0.0      | 76 ± 25  |

The filler is BNNT

<sup>a</sup> p refers to the p index, which describes the fractional contribution of the parallel configuration (as opposed to the series configuration)

<sup>b</sup> Volume fraction of air is determined by analyzing optical microscope photographs

<sup>c</sup> Fractional increase in the measured conductivity relative to the corresponding value obtained at 0.69 MPa curing without prepreg treatment

<sup>d</sup> With prepreg treated with ethanol for 3 s

<sup>e</sup> With prepreg treated with toluene for 3 s

<sup>f</sup> With prepreg treated with 0.021 wt% of BNNT/toluene solution for 3 s

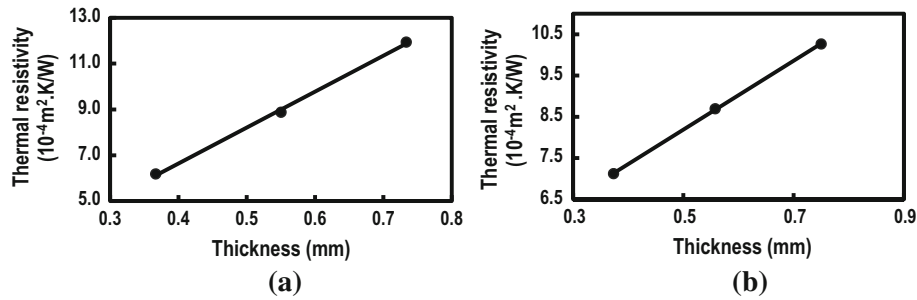


**Fig. 4** Plot of thermal resistivity versus thickness. Three thicknesses corresponding to laminates with 2, 3, and 4 laminae are shown for each type of composite. The curing pressure is 0.69 MPa. **a** Woven

composite, in the absence of prepreg treatment. **b** Woven composite with BNNT/toluene treatment of the prepreg

more influence, because both prepreg treatment and curing pressure increase result in resin removal. The prepreg treatment is more effective than increasing the curing pressure to 2.0 MPa, but is less effective than increasing the curing pressure to 4.0 MPa.

The BNNT incorporation (along with toluene treatment) further increases the thermal conductivity beyond the level provided by toluene treatment alone. The fractional increase due to BNNT incorporation, relative to the toluene-treated composite without BNNT, is 30 %.

The conductivity of the composite with filler (along with solvent treatment) is higher than that of the composite without filler but with solvent-treated prepreg. Moreover, it is higher than the values obtained without filler and with untreated prepreg, but at higher curing pressures of 2.0 and 4.0 MPa. Thus, the filler addition (along with solvent treatment) is more effective for increasing the conductivity than curing pressure increase or solvent treatment of the prepreg.

### Thermal conductivity modeling

#### Modeling the overall composite

The thermal conductivity is calculated from the component volume fractions and the component thermal conductivity values, based on the Rule of Mixtures. This rule differs between the parallel and series thermal configuration of the components [28]. For the parallel configuration, the thermal conductivity  $k_P$  of the composite without filler and without air void is given by

$$k_P = v_f k_f + v_m k_m, \tag{5}$$

where  $k_f$  and  $k_m$  are the thermal conductivities of the fibers and matrix, respectively, and  $v_f$  and  $v_m$  are the corresponding volume fractions. For the series configuration,  $k_S$  of the composite is given by

$$\frac{1}{k_S} = \frac{v_f}{k_f} + \frac{v_m}{k_m}. \tag{6}$$

For composites with air voids but without filler, the thermal conductivity can be similarly calculated. Using the parallel model,

$$k_P = v_f k_f + v_m k_m + v_a k_a, \tag{7}$$

where  $k_a$  is thermal conductivity of air (0.024 W/(m K) [29]). Using the series model,

$$\frac{1}{k_S} = \frac{v_f}{k_f} + \frac{v_m}{k_m} + \frac{v_a}{k_a}. \tag{8}$$

For the composite with both filler and air voids, the thermal conductivity can be similarly calculated. Using the parallel model,

$$k_P = v_f k_f + v_m k_m + v_a k_a + v_b k_b, \tag{9}$$

where  $k_b$  is the thermal conductivity of the filler (BNNT, 18 W/m K [30]). Using the series model,

$$\frac{1}{k_S} = \frac{v_f}{k_f} + \frac{v_m}{k_m} + \frac{v_a}{k_a} + \frac{v_b}{k_b}. \tag{10}$$

In addition to the purely series model [Eqs. (6), (8), and (10) and the purely parallel model (Eqs. (5), (7), and (9)), this work also uses models with both series and parallel units. Figure 5a shows a model with series and parallel units in series, whereas Fig. 5b) shows a model with series and parallel units in parallel. For each of Fig. 5a, b, the series and parallel units are given various fractional values of the weighting factor, which is  $\beta (\leq 1)$  for the parallel unit and  $1 - \beta$  for the series unit. For the case of Fig. 5(a), the thermal conductivity  $k$  is given by

$$\frac{1}{k} = \frac{\beta}{k_P} + \frac{1 - \beta}{k_S} \tag{11}$$

For the case of Fig. 5b, the thermal conductivity  $k$  is given by

$$k = \beta k_P + (1 - \beta) k_S \tag{12}$$

Table 4 shows a comparison of the measured and calculated thermal conductivity values for the various woven

**Fig. 5** **a** The model with parallel and series units in series. **b** The model with parallel and series units in parallel. Each of these two models involves F, M, B, and A, which represent glass fibers, matrix, BNNT, and air voids, respectively

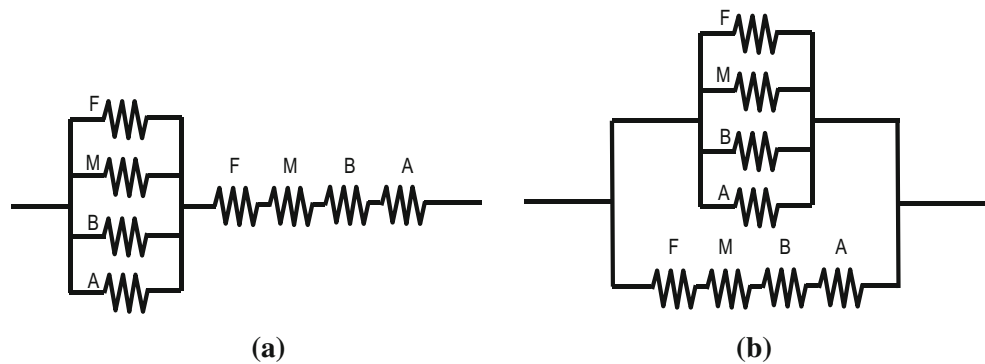


**Table 4** Comparison of the measured thermal conductivity with the calculated thermal conductivity based on various models

| Curing pressure (MPa)  | 0.69               | 0.69 <sup>a</sup>  | 0.69 <sup>b</sup>  | 0.69 <sup>c</sup> | 2.0                | 4.0                |
|--|--------------------|--------------------|--------------------|-------------------|--------------------|--------------------|
| Filler   | –                  | –                  | –                  | BNNT              | –                  | –                  |
| Measured thermal conductivity (W/(m K))  | 0.640 ± 0.041      | 0.926 ± 0.059      | 0.922 ± 0.052      | 1.20 ± 0.02       | 0.916 ± 0.012      | 1.12 ± 0.08        |
| Calculated thermal conductivity (W/(m K))  |                    |                    |                    |                   |                    |                    |
| Purely parallel configuration  | 0.80 ± 0.01        | <i>0.86 ± 0.02</i> | <i>0.91 ± 0.00</i> | <i>1.1 ± 0.1</i>  | <i>0.85 ± 0.01</i> | <i>0.89 ± 0.01</i> |
| Purely series configuration  | 0.36 ± 0.01        | 0.39 ± 0.01        | 0.26 ± 0.00        | 0.26 ± 0.00       | 0.39 ± 0.01        | 0.41 ± 0.01        |
| Ratio of the weighting factors of the parallel and series units in the equivalent circuit with the parallel and series units in series   |                    |                    |                    |                   |                    |                    |
| 0.5:0.5  | 0.50 ± 0.01        | 0.54 ± 0.01        | 0.40 ± 0.00        | 0.42 ± 0.00       | 0.53 ± 0.01        | 0.57 ± 0.01        |
| 0.6:0.4  | 0.54 ± 0.01        | 0.58 ± 0.01        | 0.45 ± 0.00        | 0.48 ± 0.01       | 0.58 ± 0.01        | 0.61 ± 0.01        |
| 0.7:0.3  | 0.59 ± 0.01        | 0.63 ± 0.01        | 0.52 ± 0.00        | 0.56 ± 0.01       | 0.63 ± 0.01        | 0.66 ± 0.01        |
| 0.8:0.2  | <i>0.64 ± 0.01</i> | 0.70 ± 0.01        | 0.61 ± 0.00        | 0.67 ± 0.02       | 0.69 ± 0.01        | 0.73 ± 0.01        |
| 0.9:0.1  | 0.72 ± 0.01        | 0.77 ± 0.02        | 0.73 ± 0.00        | 0.85 ± 0.03       | 0.76 ± 0.01        | 0.80 ± 0.01        |
| Ratio of the weighting factors of the parallel and series units in the equivalent circuit with the parallel and series units in parallel |                    |                    |                    |                   |                    |                    |
| 0.5:0.5  | 0.58 ± 0.01        | 0.63 ± 0.01        | 0.58 ± 0.00        | 0.70 ± 0.03       | 0.62 ± 0.01        | 0.65 ± 0.01        |
| 0.6:0.4  | 0.63 ± 0.01        | 0.67 ± 0.01        | 0.65 ± 0.00        | 0.79 ± 0.04       | 0.67 ± 0.01        | 0.70 ± 0.01        |
| 0.7:0.3  | 0.67 ± 0.01        | 0.72 ± 0.01        | 0.72 ± 0.00        | 0.88 ± 0.05       | 0.71 ± 0.01        | 0.75 ± 0.01        |
| 0.8:0.2  | 0.72 ± 0.01        | 0.77 ± 0.02        | 0.78 ± 0.00        | 0.97 ± 0.05       | 0.76 ± 0.01        | 0.80 ± 0.01        |
| 0.9:0.1  | 0.76 ± 0.01        | 0.81 ± 0.02        | 0.85 ± 0.00        | <i>1.1 ± 0.1</i>  | 0.81 ± 0.01        | 0.85 ± 0.01        |

The composites involve woven glass fibers. The calculated thermal conductivity values based on 12 models are shown. These models are the purely parallel configuration, the purely series configuration, 5 models with the parallel and series units in series (Fig. 5a), and 5 units with the parallel and series units in parallel (Fig. 5b). Calculated values that are closest to the corresponding measured values are shown in italics

<sup>a</sup> With prepreg treated with ethanol for 3 s

<sup>b</sup> With prepreg treated with toluene for 3 s

<sup>c</sup> With prepreg treated with 0.021 wt% of BNNT/toluene solution for 3 s

fiber composites. The calculated values are based on 12 models, which all involve the Rule of Mixtures for the components (fiber, matrix, BNNT, and air voids, as applicable) in the composite. These models include (i) the purely parallel model, (ii) the purely series model, (iii) 5 models involving Fig. 5a, with various weighting factors for the parallel and series units shown in Fig. 5a, and (iv) 5 models involving Fig. 5b, with various weighting factors for the parallel and series units shown in Fig. 5b. The model that gives the closest fit between the corresponding

measured and calculated conductivity values has the calculated value indicated in italics in Table 4. The purely series model is worst, with the calculated values being very low from the corresponding measured values. The purely parallel model is the best for most cases, with the calculated values being close to the corresponding measured values. Among the models involving both parallel and series units, whether these units are in series or in parallel, the greater is the weighting factor for the parallel unit, the better is the model. The purely parallel model is the most

effective for all cases, except that the model involving Fig. 5a and the weighting factors for the parallel and series units at the ratio 0.8:0.2 gives the best fit for the unmodified composite prepared at a curing pressure of 0.69 MPa. In particular, for the composite with BNNT, the model involving Fig. 5b and the highest parallel to series unit ratio of 0.9:0.1 gives as good a fit to the corresponding measured conductivity value as the purely parallel model. Thus, for all the cases, models involving purely or primarily the parallel configuration give the best fit to the measured values.

Table 5 shows the contributions of the various components to the calculated thermal conductivity, with the calculation based on the Rule of Mixtures with the components in parallel in the through-thickness direction. The Rule of Mixtures with the components in series does not give reasonable results, as expected due to the insulating air being modeled as a film in the plane direction. In the parallel model, the air is modeled as a column in the through-thickness direction. This is not realistic, due to the fact that the air voids are distributed at the interlaminar interface. In spite of this shortcoming, the parallel model provides approximate information on the relative contributions by the various components. As shown in Table 5, the main contributor to the thermal conductivity of the composite is the fiber. The contribution by the matrix is much smaller and the contributor by the air is even smaller. For the composite with the BNNT filler, the contribution by the filler is much greater than that of the matrix, but it is smaller than that of the fiber.

Due to the fact that the fibers are oriented in-plane, the series thermal configuration for the two components would intuitively be expected to apply. However, it does not apply. This means that the fiber–fiber contacts in the through-thickness direction, as enabled by the fact that the fibers are not perfectly straight, govern the through-thickness thermal conductivity. In other words, the through-thickness conduction path is through one fiber–fiber contact after another, thereby making the fibers effectively (roughly) in the through-thickness direction from the viewpoint of thermal conduction. This implies that the fiber–fiber interfacial thermal resistance contributes significantly to the thermal resistance of the composite. This finding is consistent with prior work on carbon fiber

composites, though the prior work did not consider the parallel and series configurations [23].

The in-plane thermal conductivity of continuous glass fiber composites may be modeled by using the Rule of Mixtures with the fibers and matrix in parallel, due to the continuity of the fibers in the in-plane direction. Since the equation for the calculation is identical for the in-plane and through-thickness directions, the calculated in-plane values are identical to those with the fibers and matrix in parallel in the through-thickness direction, as shown in Table 3. This means that the composites are similar in the thermal conductivity in the through-thickness and in-plane directions. This essential isotropy is consistent with the previously reported essential isotropy for aligned short glass fiber composites [7]. The scientific origin of the essential isotropy found in this work for continuous glass fiber composites relates to the high degree of fiber–fiber contact in the through-thickness direction. This explanation is in contrast to the prior explanation in terms of the isotropy within a fiber [7].

The relative contributions of the parallel and series configurations to the measured thermal conductivity can be calculated using the equation

$$\text{Measured conductivity} = p(\text{calculated conductivity for the parallel configuration}) + (1 - p)(\text{calculated conductivity for the series configuration}), \tag{13}$$

where  $p$  is the fractional contribution by the parallel configuration. The exact parallel configuration and the exact series configuration are two extreme states. The actual state is between them. Conduction involving the parallel configuration requires through-thickness fiber–fiber contacts, whereas conduction involving the series configuration does not require these contacts. These contacts are due to the fiber waviness in the through-thickness direction. A degree of fiber waviness always exists, regardless of the fiber layout configuration. In the series configuration for through-thickness conduction, the conduction path is through the fibers in the transverse direction of the fibers and through the matrix between adjacent fibers. In contrast, in the parallel configuration, the conduction path is through the fiber–fiber contact points and through the part of the

**Table 5** Contribution of air voids to the calculated thermal conductivity of the composite treated with toluene or BNNT/toluene

| Composite            | Thermal conductivity (W/m K) contribution of each component |               |               |               |
|----------------------|---|---------------|---------------|---------------|
|                      | Fiber   | Matrix        | Filler        | Air           |
| Toluene treated      | 0.853 ± 0.003   | 0.057 ± 0.001 | –             | 0.001 ± 0.000 |
| BNNT/toluene treated | 0.853 ± 0.003   | 0.054 ± 0.001 | 0.236 ± 0.070 | 0.001 ± 0.000 |

The calculation is based on the Rule of Mixtures with the components in parallel. The Rule of Mixtures with the components in series does not give reasonable results

fiber between adjacent contact points. Due to the relatively low thermal conductivity of the matrix, the heat flow path within the fibers is primarily along the axis of the fibers rather than in the direction transverse to the fiber axis, as illustrated in Fig. 6. A larger number of contact points within the same volume would allow the heat flow path to undergo less deviation (i.e., less detour) from the through-thickness direction, thereby decreasing the length of the heat flow path. The extreme case of exact parallel configuration can only be achieved when the number of contact points is so large that the detour of the heat flow path from the through-thickness direction is negligible. The extent of through-thickness fiber–fiber contact mainly relates to the quantity of fiber–fiber contact points, although it also relates to the quality (intimacy) of the contact. The relevant contact points are within the laminae, with essential exclusion of the fiber–fiber contact across the interlaminar interfaces, because the thermal resistivity of the interlaminar interfaces is negligible compared to that of the laminae (“Decoupled volumetric and interfacial contributions to the thermal resistivity” section).

The quantification of the extent of fiber–fiber contact by microscopy is nearly impossible, due to the low degree of through-thickness fiber waviness and the large number of contact points that are distributed throughout each lamina. The degree of fiber waviness is exaggerated in Fig. 6. The method involving the  $p$  index is a practical way of assessing and quantifying the extent of through-thickness intralaminar fiber–fiber contact. More complicated equations based on the variational approach [20] and on combinations of parallel and series models [21] have been found to be less suitable.

The  $p$  index increases monotonically with increasing curing pressure, as observed for the woven composites

(Table 3). This means that the degree of through-thickness fiber–fiber contact increases with increasing curing pressure, so that the parallel model becomes more dominating as the curing pressure increases. The  $p$  index (Table 3) exceeds 0.5 for all the composites and exceeds 0.8 for all but one composite. This means that the parallel configuration dominates over the series configuration. In other words, the actual situation corresponds to a state between the exact parallel configuration and the exact series configuration, such that it is closer to the exact parallel extreme than the exact series extreme. In Fig. 6, the thick line in the through-thickness direction is the path of the part of the heat flow that corresponds to the series configuration, whereas the thin line is the path of the part of the heat flow that corresponds to the parallel configuration. In the parallel configuration, multiple paths akin to the thin line in Fig. 6 are thermally in parallel. In the actual situation in which both parallel and series configurations contribute, the two paths described by the thick and thin lines in Fig. 6 are thermally in parallel, such that the overall direction of each path is in the through-thickness direction and the path with the smaller thermal resistance dominates. The relatively high thermal resistance of the path corresponding to the series configuration is mainly due to the low thermal conductivity of the matrix, which constitutes a substantial part of the path. A smaller degree of fiber waviness would cause the part of the series configuration path through the matrix to be shorter, thus decreasing the thermal resistance of the series configuration path. In addition, a smaller degree of fiber waviness would decrease the number of fiber–fiber contact points in the same volume of the composite, thus increasing the extent of detour and the thermal resistance of the parallel configuration path. Hence, a smaller degree of fiber waviness would enhance the series configuration contribution and reduce the parallel configuration contribution.

The  $p$  index exceeds 0.8 for all the composites except the woven one made at the low curing pressure of 0.69 MPa in the absence of prepreg treatment. This suggests that the weaving makes through-thickness fiber–fiber contact more difficult, probably because the woven geometry limits the degree of through-thickness fiber waviness. The woven configuration causes one fiber bundle to hold down another fiber bundle in the through-thickness direction, thereby limiting the local change in fiber orientation toward the through-thickness direction that is important for achieving through-thickness fiber–fiber contact. Thus, the relatively low thermal conductivity of the woven composite made at the low curing pressure of 0.69 MPa in the absence of prepreg treatment is not just due to the relatively low fiber volume fraction, but is also due to the difficulty for achieving through-thickness fiber–fiber contact.

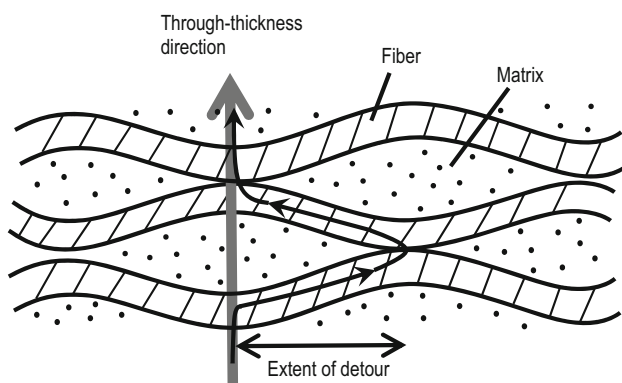


**Fig. 6** Schematic illustration of the heat flow path associated with through-thickness thermal conduction. The dotted regions are the matrix. The hatched regions are the fibers. *Thin line*: the dominant heat flow path for the parallel configuration. *Thick line* (through-thickness direction): the dominant heat flow path for the series configuration. The degree of fiber waviness is exaggerated in this drawing

The prepreg treatment increases the  $p$  index, whether the composite is unidirectional, crossply, or woven. This is because the prepreg treatment removes the excess resin on the prepreg surface, thereby enhancing the through-thickness fiber–fiber contact at least in the surface region of each lamina.

The BNNT incorporation increases the  $p$  index, relative to the composite without BNNT but with toluene treatment. This is probably because the BNNT incorporation enhances the fiber waviness, as suggested by the higher air void content when the BNNTs are present.

The fact that some of the values of the  $p$  index exceed 1 is due to the limited accuracy of the calculated thermal conductivity—partly a consequence of the likely inaccuracy in the value of the thermal conductivity of the glass fiber. For example, in the case of the  $p$  index of 1.1 (woven, 2.0 MPa) (Table 3), this value would be reduced to 1.00 if the conductivity of the glass fiber is increased by 7.7 %. Another source of the inaccuracy probably relates to the value of the conductivity of the matrix.

For the same fabrication condition shown in Table 3, the  $p$  index is similar for the unidirectional, crossply, and woven composites, except for the woven composite made at the low curing pressure of 0.69 MPa in the absence of the prepreg treatment. In other words, the prepreg treatment and the increase in curing pressure from 0.69 to 2.0 MPa are more influential to the  $p$  index for the woven composite than the nonwoven composites. This is due to the relatively high matrix volume fraction in the woven composite made at the low curing pressure of 0.69 MPa in the absence of prepreg treatment.

The similarity in thermal conductivity and  $p$  index for the unidirectional and crossply composites made under the same condition is consistent with the fact that the thermal resistivity of the interlaminar interfaces is negligible (“Decoupled volumetric and interfacial contributions to the thermal resistivity” section), so that the thermal resistivity is dominated by that of the laminae. Whether the composite is unidirectional or crossply, the fibers are aligned within each lamina.

For the same fiber configuration (among the three configurations in Table 3), the  $p$  index is higher for the composite made at the lowest curing pressure of 0.69 MPa in the presence of prepreg treatment than that made at the higher curing pressure of 2.0 MPa in the absence of prepreg treatment. This is because the curing pressure increase enhances the in-plane fiber alignment within each lamina, whereas the prepreg treatment does not. Greater alignment causes less chance for through-thickness fiber–fiber contact and hence a lower value of  $p$ . However, by further increasing the curing pressure to 4.0 MPa, the  $p$  index is higher than those of all other conditions. This result for the curing pressure of 4.0 MPa is attributed to the

enhancement of the quality of each fiber–fiber contact. This enhancement causes the  $p$  index to increase, in spite of the possible decrease in the number of contacts.

For any of the three fiber configurations, increase in the curing pressure (without prepreg treatment) causes the  $p$  index to increase. This observation is consistent with the fact that, in case of continuous nonwoven carbon fiber epoxy–matrix composites, the intralaminar fiber–fiber interfacial thermal resistivity (i.e., the resistivity of all the fiber–fiber interfaces in a lamina) in the through-thickness direction decreases as the curing pressure increases [23]. The intralaminar fiber–fiber interfacial resistivity can be used as an indicator of the extent of through-thickness fiber–fiber contact. However, it is not as convenient as the  $p$  index, which is dimensionless, in serving as an indicator.

### Modeling a lamina

The thermal resistivity  $R_\ell$  of a lamina is given by

$$R_\ell = R_f + R_a, \quad (14)$$

where  $R_f$  is the thermal resistivity of all of the fibers stacked along the thickness of the lamina, and  $R_a$  is the thermal resistivity of all of the fiber–fiber contacts along the thickness of the lamina [23]. The thermal resistivity  $R_f$  is given by

$$R_f = \frac{Md}{k_f}, \quad (15)$$

where  $d$  is the fiber diameter (7  $\mu\text{m}$ ),  $M$  (28 on the average, based on cross-sectional optical microscopy, with the averaging necessitated by the woven configuration) is the number of stacked fibers in a lamina, and  $k_f$  (1.3 W/(m K)) is the transverse conductivity of a fiber. Using Eq. (13),  $R_f = 1.93 \times 10^{-4} \text{ m}^2/(\text{K}\cdot\text{W})$ .

The  $R_\ell$  is obtained from Eq. (4) and an experimentally obtained curve (Fig. 4). Hence, using Eq. (12),  $R_a$  is obtained. The  $R_\ell$  is much greater than  $R_a$  (Table 6), indicating that  $R_\ell$  is dominated by  $R_f$ .

Table 6 shows that both  $R_\ell$  and  $R_a$  are decreased by the composite modification (whether using toluene, ethanol, or BNNTs) and by curing pressure increase, but the fractional decrease is more significant for  $R_a$  than  $R_\ell$ . This means that both the composite modification and the curing pressure increase enhance the degree of through-thickness fiber–fiber contact. The higher is the curing pressure, the more is the decrease in both  $R_\ell$  and  $R_a$ . Ethanol and toluene have similar effects, but the combined use of BNNTs and toluene gives more significant effects on both  $R_\ell$  and  $R_a$ . The effects of the combined use of BNNTs and toluene are even more significant than the effects of increasing the curing pressure to 4.0 MPa. The lowest value of  $R_a$  is provided by the combined use of BNNTs and toluene.

**Table 6** The thermal resistivity of a lamina and the contribution of the fiber–fiber interfaces in the lamina to the thermal resistivity of a lamina in a woven glass fiber composite

| Composite treatment | Curing pressure (MPa) | Thermal resistivity ( $10^{-4}$ m <sup>2</sup> .K/W) |  | Fractional change in thermal resistivity due to curing pressure increase (%) |              | Fractional change in thermal resistivity due to composite modification (%) |              |
|---------------------|-----------------------|--|--|--|--------------|--|--------------|
|                     |                       | Lamina resistivity $R_\ell$                          | Intralaminar fiber–fiber interfacial resistivity $R_a$ | $R_\ell$   | $R_a$        | $R_\ell$   | $R_a$        |
| Unmodified          | 0.69                  | $2.81 \pm 0.32$                                      | $1.31 \pm 0.32$  | –  | –            | –  | –            |
| Ethanol             |                       | $2.02 \pm 0.21$                                      | $0.511 \pm 0.212$                                      | –  | –            | $-28 \pm 16$   | $-61 \pm 27$ |
| Toluene             |                       | $1.93 \pm 0.23$                                      | $0.426 \pm 0.233$                                      | –  | –            | $-31 \pm 16$   | $-67 \pm 27$ |
| BNNT/toluene        |                       | $1.53 \pm 0.00$                                      | $0.0258 \pm 0.0013$                                    | –  | –            | $-46 \pm 6$  | $-98 \pm 1$  |
| Unmodified          | 2.0                   | $1.97 \pm 0.04$                                      | $0.460 \pm 0.043$                                      | $-30 \pm 9$  | $-65 \pm 13$ | –  | –            |
| Unmodified          | 4.0                   | $1.61 \pm 0.20$                                      | $0.0971 \pm 0.202$                                     | $-43 \pm 14$   | $-93 \pm 18$ | –  | –            |

Figure 7 shows a high value of  $p$  (Table 3) correlates with a low value of  $R_a$  (Table 6). This correlation supports the validity of both models (“Modeling the overall composite” and “Modeling a lamina” sections) and reinforces the notion that the mechanism of thermal conduction involves fiber–fiber contacts in the through-thickness direction.

### Flexural testing

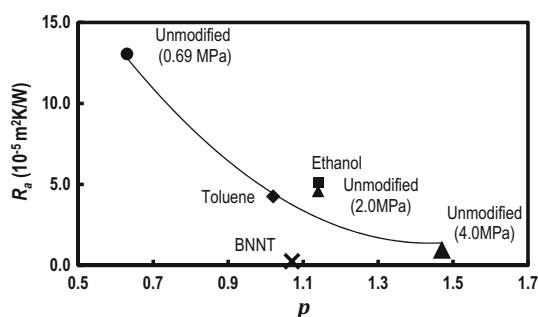
Table 7 shows that the flexural modulus is slightly decreased by the composite modification by either toluene treatment or the combination of toluene treatment and BNNT incorporation, while the strength is decreased by up to 14 %. In spite of the higher porosity in the composite treated with the combination of toluene treatment and BNNT incorporation compared to the composite with toluene treatment alone (Table 3), the strength is higher for the former. This is attributed to the strengthening effect of the BNNTs in the former. On the other hand, the ductility is increased by the modification, such that the ductility is highest for the composite modified by toluene treatment. Figure 8 shows the representative flexural stress–strain

curves of the three composite types of Table 7. The unmodified composite has no tail in the stress–strain curve, whereas the two modified composites have jagged tails. Each tail is due to a series of delamination events, as visually observed during testing. The tail is slightly larger (with the larger area under the curve) for the toluene-treated composite than the composite with both toluene treatment and BNNT incorporation. Hence, high ductility correlates with high toughness. High ductility also correlates with low strength (Table 7). Both low strength and high ductility are attributed to the greater ease of delamination.

### Comparison of glass fiber composites and carbon fiber composites

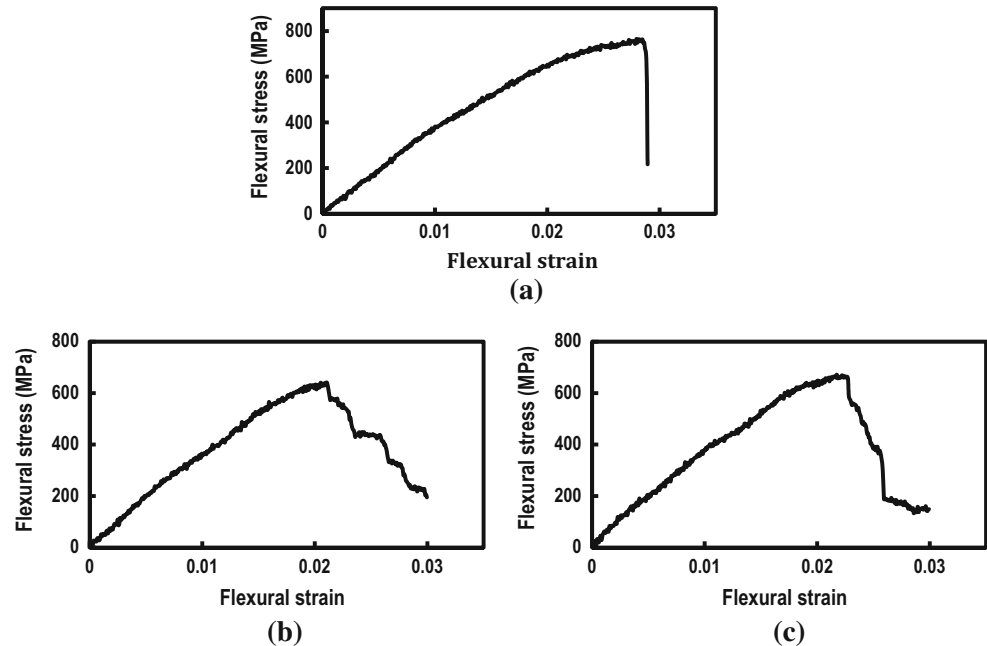
This work addresses glass fiber composites. The methodology is the same as that of prior work [23] concerning carbon fiber composites. This work and Ref. [23] use the same method of thermal conductivity measurement, including the same method of decoupling the interfacial thermal resistivity and the specimen thermal resistivity. Thus, comparison of the results on the two types of composites is appropriate.

For continuous nonwoven carbon fiber epoxy–matrix composites without prepreg treatment, Ref. [23] reported through-thickness thermal conductivity 1.09 W/(m K) for a curing pressure of 2.0 MPa. The value obtained by Ref. [23] is comparable to the value of 1.07 or 1.03 W/(m K) obtained in this work for nonwoven glass fiber composites at the same curing pressure, even though carbon fiber is much more thermally conductive than glass fiber. This similarity in thermal conductivity supports the importance of fiber–fiber contacts in affecting the conductivity. It further means that work aimed at achieving high through-thickness thermal conductivity in continuous fiber

**Fig. 7** Correlation of  $R_a$  (Table 6) and  $p$  (Table 3)

**Table 7** Flexural properties of woven glass fiber composites

| Composite treatment  | Thickness (mm) | Modulus (GPa) | Strength (MPa) | Ductility (%) |
|----------------------|----------------|---------------|----------------|---------------|
| Untreated            | 1.92 ± 0.02    | 37.4 ± 0.7    | 751 ± 13       | 2.04 ± 0.11   |
| Toluene treated      | 1.88 ± 0.02    | 35.9 ± 0.5    | 643 ± 13       | 2.76 ± 0.06   |
| BNNT/toluene treated | 1.88 ± 0.02    | 36.5 ± 0.6    | 685 ± 13       | 2.25 ± 0.05   |

**Fig. 8** Representative stress–strain curves of woven glass fiber epoxy–matrix composites. **a** Untreated composite. **b** Composite with toluene treatment. **c** Composite with toluene treatment and BNNT incorporation

polymer–matrix composites should focus on the fiber–fiber contacts rather than the choice of fibers. The number of fiber–fiber contacts increases with increasing degree of fiber waviness, as illustrated in Fig. 6. Fiber waviness is disadvantageous for the mechanical properties of the composites, though this disadvantage is not a significant concern in case of nonstructural applications such as printed wiring boards.

The  $R_\ell$  values in Table 6 for glass fiber composites are higher than those of carbon fiber epoxy–matrix composites of prior work [23], as expected, due to the higher thermal conductivity of carbon fibers compared to glass fibers. However, the  $R_a$  values are comparable for glass fiber composites and carbon fiber composites.

The fractional decrease in  $R_\ell$  due to composite modification is comparable for the glass fiber composites of this work and the carbon fiber composites of prior work [23], but the fractional decrease in  $R_a$  is greater for the glass fiber composites than the carbon fiber composites. As a result, the fractional increase in the thermal conductivity due to the composite modification is higher for the glass fiber composites of this work than the carbon fiber composites of prior work [23].

Since the thermal conductivity of carbon fiber is higher than that of glass fiber, the role of fiber–fiber

contacts is expected to be even more dominant in case of carbon fiber composites. Calculation using the series and parallel models of this paper shows that, for the carbon fiber composites [23], the measured thermal conductivity obeys the series model much more closely than the parallel model. In the absence of fillers, the  $p$  index is only 0.063 and 0.125 for curing pressures of 0.1 and 2.0 MPa, respectively, as calculated in this work using the results of Ref. [23]. As in the case of the glass fiber composites of this work, the  $p$  index of the carbon fiber composites increases with increasing curing pressure. This is attributed to the high thermal conductivity (7 W/(m K)) of the carbon fibers compared to the glass fibers and the consequent greater dominant contribution of the fiber–fiber contacts to the thermal resistance. This dominance causes the series configuration to provide a lower resistance path than the parallel configuration. Thus, the mechanism of through-thickness thermal conduction differs between glass fiber composites and carbon fiber composites.

For both glass fiber composites and carbon fiber composites, the plot of thermal resistivity versus thickness is linear. This indicates that the interlaminar interface contribution to the thermal resistivity is negligible compared to the lamina contribution for both types of composite.

## Further discussion

For all the composites studied in terms of the through-thickness thermal conductivity, the thermal resistivity of the interlaminar interface is negligible compared to that of each lamina. The lamina resistivity is dominated by the resistivity of the fibers in the lamina. Though the resistivity of the fiber–fiber interfaces in a lamina is the minority contributor to the lamina resistivity, it decreases significantly with increasing curing pressure and with composite modification by solvent or filler (BNNTs). The mechanism of thermal conductivity increase due to the composite modification or the curing pressure increase relates to the increase in the degree of fiber–fiber contact within each lamina in the composite. The higher is the curing pressure, the greater is the degree of fiber–fiber contact within a lamina, as expected.

Even though the composite modification is incurred at the interlaminar interface (due to the modification being performed on the prepreg surface prior to composite fabrication), the modification affects the structure within each lamina in the composite. In case of modification using a solvent (ethanol or toluene), the solvent apparently does not merely remove a part of the resin from the prepreg surface, but it probably removes a part of the resin from the interior of the prepreg sheet also. In case of modification using BNNTs, the BNNTs reside at the interlaminar interface, but they probably increase the degree of fiber waviness in each lamina, thereby increasing the degree of fiber–fiber contact.

Prior work by others showed an increase of up to 140 % [8] or 62 % [9] in the in-plane thermal conductivity of glass fiber polymer–matrix composites due to the addition of CNTs to the matrix and no increase (with consideration of the large error bars) [10] in the through-thickness conductivity due to the addition of carbon nanofibers to the matrix. By using BNNT as the filler (along with solvent treatment of the prepreg), this work has achieved  $(88 \pm 15) %$  increase in the through-thickness thermal conductivity. By increasing the curing pressure, this work has achieved up to  $(76 \pm 25) %$  increase in the through-thickness thermal conductivity. This means that both BNNT addition (along with solvent treatment of the prepreg) and curing pressure increase are more effective than CNF addition for enhancing the through-thickness conductivity. The difference between this work and prior work is partly due to the fact that the glass fibers (0.05 W/(m K)) used in prior work [8] have much lower thermal conductivity than the matrix (0.18 W/(m K)). As a consequence, the matrix is dominant in providing thermal conduction and hence its modification by CNT addition gives a large effect on the conductivity of the composite. The difference is also partly because the fiber content in the prior work is only

25 vol% [8], 48 vol% [9] or 30–35 vol% [10], compared to 55 vol% in this work. A lower fiber content means a higher matrix content, which makes the matrix modification more influential. In contrast, this work addresses the through-thickness thermal conductivity and involves a typical situation in which the fibers are considerably more conductive than the matrix and the glass fiber content is high for providing high mechanical performance.

The highest in-plane thermal conductivity of glass fiber polymer–matrix composites previously reported is 0.44 W/(m K) [8] or 0.43 W/(m K) [9], as obtained by the addition of CNT to the matrix. The through-thickness conductivity has previously been reported to be 0.377 W/(m K) [11] and 0.38 W/(m K) [22] for unmodified glass fiber composites containing 60 and 57 vol% glass fibers, respectively, and 0.19 W/(m K) for a glass fiber (30–35 vol%) composite with carbon nanofibers added to the matrix [10]. For FR-4, the value is 0.29 W/(m K). In contrast, the through-thickness conductivity obtained in this work is up to 1.2 W/(m K), which is higher than all of the previously reported values for glass fiber composites. The glass fiber volume fraction of this work is comparable to those of prior work [11, 22]. The high thermal conductivity values obtained in this work compared to the other prior work are at least partly due to the decoupling of the contact thermal resistivity and the specimen thermal resistivity by using the method illustrated in Fig. 4. In contrast, prior work [8–11, 22] did not perform the decoupling.

Glass fiber polymer–matrix composites are lightweight construction materials, for which the thermal insulation ability is desired for energy conservation. Therefore, the decrease of the thermal conductivity is of practical interest. The findings of this work indicate that the decrease of the through-thickness thermal conductivity of these composites may be accomplished by decreasing the extent of fiber–fiber contact without increasing the fiber volume fraction. Increasing the curing pressure decreases the extent of fiber–fiber contact, but it increases the fiber volume fraction as well due to resin squeeze-out. Therefore, other methods of decreasing the extent of fiber–fiber contact should be considered.

When the conduction path mainly involves that of the parallel configuration, as in the case of the glass fiber composites, the  $p$  index is high. When the conduction path mainly involves that of the series configuration, as in the case of the carbon fiber composites, the  $p$  index is low. Within each case, the  $p$  index relates to the extent of fiber–fiber contact. However, the extent of fiber–fiber contact in case of dominance by the series configuration (i.e., the case of a low  $p$  index) is not necessarily lower than that in case of dominance by the parallel configuration (i.e., the case of a high  $p$  index). This is because, when the series configuration dominates, the effect of the fiber–fiber contact is

relatively small, even though the extent of contact may be high. However, within the category of parallel dominance or within the category of series dominance, the  $p$  index relates to the extent of fiber–fiber contact.

## Conclusion

This paper provides new understanding of the through-thickness thermal conduction in glass fiber polymer–matrix composites, in addition to providing methods of modifying the composite for enhancing this conductivity. The findings are significant from both scientific and technological viewpoints.

The thermal resistivity of the interlaminar interface is negligible compared to that of each lamina. The lamina resistivity is dominated by the resistivity of the fibers in the lamina. Nevertheless, the resistivity of the fiber–fiber interfaces in a lamina decreases significantly with increasing curing pressure and with composite modification by solvent or filler (BNNTs). The thermal conduction occurs mainly through through-thickness fiber–fiber contacts, so that the conductivity mainly obeys the Rule of Mixtures for the parallel configuration of the fibers and matrix rather than that for the series configuration. The  $p$  index is introduced to describe the mechanism of through-thickness thermal conduction. It is based on the relative contributions of the parallel and series configurations to the conductivity and mathematically corresponds to the fractional contribution by the parallel configuration. A high value of the  $p$  index correlates with a low value of  $R_a$ , which is the thermal resistivity of the fiber–fiber contacts in a lamina.

The through-thickness thermal conductivity of the composites is comparable to (though smaller than) the axial thermal conductivity of the individual fiber. The composites are similar in the thermal conductivity in the through-thickness and in-plane directions. This is enabled by the fiber–fiber contacts in the through-thickness direction providing an effective thermal conduction path. The mechanism of thermal conductivity increase due to the composite modification or the curing pressure increase relates to the increase in the degree of fiber–fiber contact within each lamina in the composite.

At the low curing pressure of 0.69 MPa in the absence of prepreg treatment, the  $p$  index and the thermal conductivity are lower for the woven composite than the nonwoven composites. Increase in the curing pressure from 0.69 to 4.0 MPa or treatment of the prepreg by a solvent that partially dissolves the resin on the prepreg surface increases the  $p$  index and the thermal conductivity for both woven and nonwoven composites. This is due to the increase in the degree of fiber–fiber contact in each lamina

and the associated decrease in the thermal resistivity of the fiber–fiber interfaces in the lamina.

The prepreg treatment using a solvent increases the  $p$  index and the thermal conductivity by similar extents as the curing pressure increase to 2.0 MPa, whether the composite is woven or not. However, the curing pressure increase to 4.0 MPa increases the  $p$  index and the thermal conductivity more significantly than the prepreg solvent treatment. The addition of BNNTs to the interlaminar interface (along with toluene treatment) increases the thermal conductivity of the composite more significantly than curing pressure increase or prepreg solvent treatment and decreases  $R_a$  as significantly as the highest curing pressure of 4.0 MPa. Increase in the curing pressure and prepreg solvent treatment increase the  $p$  index and the thermal conductivity of the woven composite more significantly than those of the nonwoven composites, due to the relatively high matrix volume fraction of the woven composite made at the low curing pressure in the absence of prepreg treatment.

The highest thermal conductivity (1.2 W/(m K)) is provided by the combined use of filler (BNNTs) incorporation and solvent (toluene) treatment of the prepreg. This value is higher than all of the previously reported values for glass fiber composites. For the unmodified composite, the thermal conductivity is 0.6 W/(m K). This method of increasing the thermal conductivity is more effective than that involving the increase of the curing pressure. The composite modification by solvent treatment and/or BNNT incorporation decreases the flexural strength and modulus slightly, while the ductility is increased.

The thermal conductivity is higher for the nonwoven composites (unidirectional or crossply) than the woven composite when the composites are fabricated under the same usual condition, i.e., the curing pressure (0.69 MPa) and the absence of prepreg treatment. The thermal conductivity is increased by 90 % by BNNT incorporation (along with solvent treatment of the prepreg), up to 80 % through curing pressure increase and up to 50 % through solvent treatment. In contrast to prior methods [8–12], these methods of thermal conductivity enhancement do not affect the electrical insulation ability of the composites. The woven composite gives greater fractional increases than the nonwoven ones. Unidirectional and crossply composites exhibit similar values of the thermal conductivity, because the interlaminar interface contributes negligibly to the thermal resistivity.

The above points apply to glass fiber composites. In contrast to the glass fiber composites, carbon fiber composites obey the series model much more closely than the parallel model, due to the relatively high thermal conductivity of the carbon fibers compared to the glass fibers. The effect of composite modification on the through-thickness

thermal conductivity is lower for carbon fiber composites than glass fiber composites, due to the smaller fractional decrease in the intralaminar fiber–fiber contact thermal resistivity for the former. In spite of the higher thermal conductivity of carbon fibers compared to glass fibers, the through-thickness thermal conductivity is comparable for the two types of composite.

#### Compliance with ethical standards

**Conflict of Interest** The authors declare that they have no conflict of interest.

#### References

- Xu Y, Chung DDL (2000) Increasing the thermal conductivity of boron nitride and aluminum nitride particle epoxy–matrix composites by particle surface treatment. *Compos Interfaces* 7(4):243–256
- Zhang X, Lin Z, Li B, Tan S (2011) Improved thermal conductivity of composite particles filled epoxy resin. *Adv Mater Res* 217–218:439–444
- He Y, Wu X, Chen Z (2011) Thermal conductivity of composite silicone rubber filled with graphite/silicone carbide. *Adv Mater Res* 221:382–388
- Zhou Y, Wang H, Xiang F, Zhang H, Yu K, Chen L (2011) A poly(vinylidene fluoride) composite with added self-passivated microaluminum and nanoaluminum particles for enhanced thermal conductivity. *Appl Phys Lett* 98(18):182906/1–182906/3
- Azar K, Graebner JE (1996) Experimental determination of thermal conductivity of printed wiring boards. In: Proceedings of the twelfth IEEE SEMI-THERM symposium, pp 169–182
- Diez-Pascual AM, Ashrafi B, Naffakh M, Gonzalez-Dominguez JM, Johnston A, Simard B, Martinez MT, Gomez-Fatou MA (2011) Influence of carbon nanotubes on the thermal, electrical and mechanical properties of poly(ether ether ketone)/glass fiber laminates. *Carbon* 49(8):2817–2833
- Kalaprasad G, Pradeep P, Mathew G, Pavithran C, Thomas S (2000) Thermal conductivity and thermal diffusivity analyses of low-density polyethylene composites reinforced with sisal, glass and intimately mixed sisal/glass fibers. *Compos Sci Technol* 60(16):2967–2977
- Wang S, Qiu J (2010) Enhancing thermal conductivity of glass fiber/polymer composites through carbon nanotubes incorporation. *Compos B* 41:533–536
- Ashrafi B, Diez-Pascual AM, Johnson L, Genest M, Hind S, Martinez-Rubi Y, Gonzalez-Dominguez JM, Martinez MT, Simard B, Gomez-Fatou MA, Johnston A (2012) Processing and properties of PEEK/glass fiber laminates: effect of addition of single-walled carbon nanotubes. *Compos A* 43:1267–1279
- Clark III RL, Skinner M, Farah B, Farris J, Hsiao K, Parker MR (2008) Thermal and electrical conductivities characterization of CNF-modified glass fiber/polyester composite. In: SAMPE conference proceedings, vol 53, pp 152/1–152/11
- Eihusen J, Peters AR (1999) Characterization of the transverse thermal conductivity of interplay hybrid composite laminates. In: 31st international SAMPE technical conference, pp. 211–220
- Zimmer M, Liang R, Wang B (2008) Thermal management of increasing through-thickness thermal conductivity of fiber-reinforced composites. In: Proceedings of the NATAS 36th annual conference on thermal analysis and applications, pp. 59/1–59/9
- Wan B, Yue K, Zheng L, Zhang X (2011) The effective thermal conductivity of composite materials with spherical dispersed phase. *Adv Mater Res* 239–242(Pt. 3):1870–1874
- Mercier S, Molinari A, El Mouden M (2000) Thermal conductivity of composite material with coated inclusions: applications to tetragonal array of spheroids. *J Appl Phys* 87(7):3511–3519
- Marcos-Gomez D, Ching-Lloyd J, Elizalde MR, Clegg WJ, Molina-Aldareguia JM (2010) Predicting the thermal conductivity of composite materials with imperfect interfaces. *Compos Sci Technol* 70(16):2276–2283
- Yue C, Zhang Y, Hu Z, Liu J, Cheng Z (2010) Modeling of the effective thermal conductivity of composite materials with FEM based on resistor networks approach. *Microsyst Technol* 16(4):633–639
- Holotescu S, Stoian FD (2009) Evaluation of the effective thermal conductivity of composite polymers by considering the filler size distribution law. *J Zhejiang Univ Sci A* 10(5):704–709
- Xu Y, Tanaka Y, Murata M, Kamihira K, Yamazaki M, Yagi K (2005) Effect of reinforcement nonuniformity on effective thermal conductivity of composite. *Mater Trans* 46(8):1786–1789
- Chung PW, Tamma KK, Namburu RR (2001) Homogenization of temperature-dependent thermal conductivity in composite materials. *J Thermophys Heat Transf* 15(1):10–17
- Hashin Z (1970) Theory of composite materials. In: Wendt FW, Liebowitz H, Perrone N (eds) *Mechanics of composite materials*. Pergamon, Oxford, pp 202–242
- Lim T (2002) Unified practical bounds for the thermal conductivity of composite materials. *Mater Lett* 54:152–157
- Mutnuri B, Liang R, Ganga RH (2006) Thermal conductivity characterization of FRP composites: experimental. In: 64th Annual technical conference—society of plastics engineers, pp 143–147
- Han S, Chung DDL (2011) Increasing the through-thickness thermal conductivity of carbon fiber polymer–matrix composite by curing pressure increase and filler incorporation. *Compos Sci Technol* 71(16):1944–1952
- Zhi C, Bando Y, Tang C, Golberg D (2010) Boron nitride nanotubes. *Mater Sci Eng R* 70(3–6):92–111
- Kalay S, Yilmaz Z, Sen O, Emanet M, Kazanc E, Culha M (2015) Synthesis of boron nitride nanotubes and their applications, Beilstein. *J. Nanotechnol* 6:84–102
- Chang CW, Han W, Zettl A (2005) Thermal conductivity of B–C–N and BN nanotubes. *Appl Phys Lett* 86(17):173102
- Ghazizadeh M, Estevez JE, Kelkar AD, Ryan JG (2014) Mechanical properties prediction of hydrogenated boron nitride nanotubes using molecular dynamic simulations. *JSM Nanotechnol Nanomed* 2(2):1030
- Chung DDL (2010) *Composite materials*, 2nd edn. Springer, New York, pp 294–295
- Wilkes K, Dinwiddie R, Graves R (1996) *Thermal conductivity*, vol 23. CRC Press, Boca Raton, pp 604–607
- Tang C, Bando Y, Liu C, Fan S, Zhang J, Ding X, Golberg D (2006) Thermal conductivity of nanostructured boron nitride materials. *J Phys Chem B* 110(21):10354–10357